Techniques for Polarization-Independent Cross-Phase Modulation in Nonlinear Birefringent Fibers

Reza Salem, *Member, IEEE*, Anthony S. Lenihan, *Member, IEEE*, Gary M. Carter, *Senior Member, IEEE*, and Thomas E. Murphy, *Senior Member, IEEE*

(Invited Paper)

***Abstract*—We present a theoretical, numerical, and experimental investigation of the polarization dependence of cross-phase modulation in nonlinear birefringent fibers. Two new methods are described for producing a polarization-independent spectral shift through cross-phase modulation of a weak probe signal by a co-propagating strong optical pulse. The birefringence of the fiber and spectral separation between the pump and probe signals are shown to play a critical role in determining the polarization dependence of the cross-phase modulation process. The methods are experimentally verified in two different highly nonlinear fibers, and are used to achieve polarization-independent optical switching at speeds of up to 160 Gb/s.**

***Index Terms*—Birefringence, demultiplexing, nonlinear optics, optical fiber polarization, optical propagation in nonlinear media, optical signal processing, polarization, ultrafast processes in fibers.**

I. Introduction

CROSS-PHASE modulation is a third-order nonlinear process in which a strong optical pump signal imparts a phase or frequency modulation on a weaker probe signal. This phase modulation can be sensed either through an interferometric measurement or by observing the spectral shift induced by a time-varying optical pump signal. In fiber-optic communication systems, cross-phase modulation has applications that include all-optical switching [1]–[5], wavelength conversion [6], [7], signal regeneration [8], [9], and optical sampling [10]. Because it is an ultrafast nonlinear effect, cross-phase modulation could perform these functions at speeds beyond what can be attained with electrical photodetection and circuitry. One obstacle that has historically prevented optical signal processing techniques from replacing electronic signal processing is the polarization dependence of nonlinear optical processes like cross-phase modulation. Since the polarization state cannot be accurately controlled or predicted in most fiber optic transmission systems, it is important to develop polarization-independent ways to exploit this nonlinear optical process.

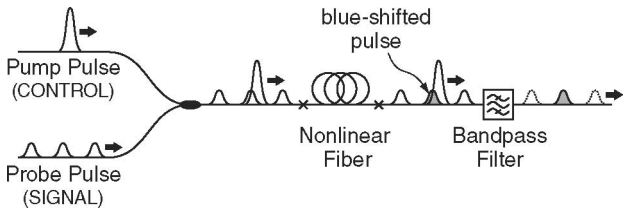

Fig. 1. Diagram showing how cross-phase modulation and spectral filtering can be used to construct an optical switch.

Fig. 1 depicts one way in which cross-phase modulation can be used to build an optical switch. In this example, the trailing edge of a strong pump signal coincides with a weaker probe pulse traveling in a nonlinear fiber. The pump pulse imposes a time-varying phase shift on the weaker probe, which causes a blueshift of the probe pulse [11]. (Conversely, the leading edge of the pump pulse would instead produce a redshift.) A spectral filter is then used to isolate the frequency-shifted portion of the signal. In this way, the pump pulse can act as an optical gating signal that controls whether the probe pulse is transmitted through the bandpass filter. The efficiency of this spectral shifting process depends on the polarization states of both optical signals, as well as the birefringence of the nonlinear fiber.

In most cases, the pump signal is locally generated and can have a prescribed polarization state. One question to be addressed in this paper is how the pump polarization, power, and wavelength should be chosen in order to minimize or eliminate the dependence on the (unknown) signal polarization state.

In theory, polarization-independent nonlinear interactions can be achieved if the pump signal is circularly polarized, but in practice, the residual birefringence of the fiber makes it difficult to maintain a circular polarization state over the length of the fiber. One method that has been successfully employed to maintain circular polarization in longer fibers is to twist the fiber either during or after fabrication [12]–[15]. Another method to overcome the polarization dependence is polarization diversity, in which the pump is split into two orthogonal states that independently interact with the data [16]–[20]. A related approach is to depolarize the pump pulse train, which requires a fiber delay that is longer than the coherence length of the pump laser [21]. In fibers that are significantly longer than the birefringence

Manuscript received October 31, 2007; revised December 17, 2007. This work was supported by the Laboratory for Physical Sciences, College Park, MD.

R. Salem was with the Department of Electrical and Computer Engineering, University of Maryland, College Park, MD 20742 USA. He is now with Cornell University, Ithaca, NY 14850-2488 USA (e-mail: reza.salem@gmail.com).

A. S. Lenihan was with the Department of Computer Science and Electrical Engineering, University of Maryland Baltimore County, Baltimore, MD 21250 USA. He is now with Ziva Corporation, San Diego, CA 92121 USA (e-mail: aslenihan@ieee.org).

G. M. Carter is with the Department of Computer Science and Electrical Engineering, University of Maryland Baltimore County, Baltimore, MD 21250 USA (e-mail: gary@lps.umd.edu).

T. E. Murphy is with the Department of Electrical and Computer Engineering, University of Maryland, College Park, MD 20742 USA (e-mail: tem@lps.umd.edu).

Digital Object Identifier 10.1109/JSTQE.2007.915391

TABLE I
LIST OF THE PARAMETERS FOR THE TWO HIGHLY NONLINEAR FIBERS (HNLF 1 AND HNLF 2) CONSIDERED IN THIS PAPER IN COMPARISON TO STANDARD SINGLE MODE FIBER (SMF-28)

Parameter	HNLF 1 (PCF)	HNLF 2 (Bi_2O_3)	SMF-28
γ ($W^{-1}\cdot km^{-1}$)	11	1100	1
D (ps/nm·km)	-0.5	-260	17
Loss (dB/m)	8×10^{-3}	3	2×10^{-4}
DGD[a] $\Delta\tau/L$ (fs/m)	42	75	0
L (m)	30	2	–

[a] Differential group delay, per unit length, describing the birefringence of the fiber.

correlation length, the random polarization mode dispersion can cause the polarization dependence to average out, leading to polarization-independent operation [22].

II. HIGHLY NONLINEAR FIBERS

Many of the earlier experiments on polarization dependence in optical fibers have been hindered by the relatively long fiber lengths required to obtain a significant nonlinear interaction. Effects like strain and microbending make it impossible to accurately control how the polarization state evolves in kilometer-length nonlinear fibers. Recently, there has been much progress in producing optical fibers with high nonlinearity, through the use of new materials and smaller mode sizes [23]–[25]. These newer nonlinear fibers enable one to achieve a significant nonlinear interaction in only a few meters of fiber, which greatly simplifies the issue of polarization control.

Although the methods described here are general and can be applied to a variety of highly nonlinear fibers, in our experiments, we have employed two representative fibers, with parameters summarized in Table I. The first is a 30-m-long, low-dispersion photonic crystal fiber manufactured by Crystal Fibre that has a nonlinearity coefficient $11\times$ higher than that of conventional fiber [26]. The second fiber is a 2-m-long bismuth-oxide-based fiber fabricated by Asahi Glass that has a nonlinearity coefficient more than $1000\times$ higher than that of conventional fiber [27].

Although these nonlinear fibers were designed to be symmetric, they both exhibit significant linear birefringence, which is believed to be caused by unintended structural anisotropy or core ellipticity introduced during fabrication [28]. We experimentally determined the birefringence given for the two nonlinear fibers in Table I by placing each between crossed polarizers and measuring the transmitted power as a function of wavelength [29]. Fig. 2 depicts the resulting spectra for each of the fibers considered. For the 30 m photonic crystal fiber, we observe a periodic sequence of evenly spaced fringes, which indicates that the birefringent axes of the fiber do not change significantly over its length, a condition that is difficult to maintain in kilometer-length fibers. The results for the bismuth-oxide-based fiber include only two fringes making it difficult to draw a similar conclusion about the birefringence axes. However, the fiber length is short, and we observed that unspooling the fiber does not affect the fringe period. We, therefore, believe that this fiber can also be treated as one birefringent medium with uniform axes.

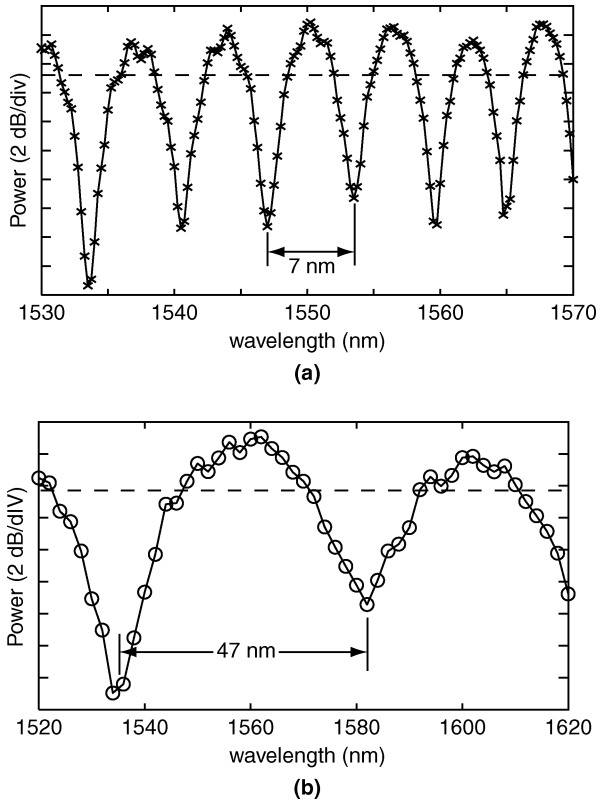

Fig. 2. Optical transmission spectrum of the two highly nonlinear fibers considered when placed between two crossed polarizers. The dashed line indicates the mean transmitted power, averaged over wavelength. (a) Transmission spectrum of HNLF-1 (a dispersion-balanced photonic crystal fiber) exhibits a periodic sequence of evenly spaced fringes suggesting that the birefringence axis is uniformly oriented throughout the 30 m length. (b) Transmission spectrum of HNLF-2, a 2 m bismuth-oxide-based small-core fiber, shows only two fringes, indicating a lower cumulative birefringence. Because of its short length, we assume that the birefringence is uniform in this fiber as well.

III. THEORY OF CROSS-PHASE MODULATION

Our analysis is based on the slowly varying amplitude approximation for the electric field. We consider the evolution of the probe signal at frequency ω_2, affected through cross-phase modulation with a strong pump signal, at frequency ω_1. We begin with an electric field comprising the two optical frequencies (pump and probe):

$$\begin{aligned}\mathbf{E}(x,y,z,t)n = {} & [\hat{\mathbf{x}}\, A_{1x}(z,t)\phi_{1x}(x,y)e^{i\beta_{1x}z} \\ & + \hat{\mathbf{y}}\, A_{1y}(z,t)\phi_{1y}(x,y)e^{i\beta_{1y}z}]e^{-i\omega_1 t} \\ & + [\hat{\mathbf{x}}\, A_{2x}(z,t)\phi_{2x}(x,y)e^{i\beta_{2x}z} \\ & + \hat{\mathbf{y}}\, A_{2y}(z,t)\phi_{2y}(x,y)e^{i\beta_{2y}z}]e^{-i\omega_2 t} \qquad (1)\end{aligned}$$

where $\phi_{nm}(x,y)$ and β_{nm} $(n = 1, 2$ and $m = x, y)$ represent the transverse electromagnetic mode and the propagation constants for each frequency and for x- and y-polarizations, respectively. $A_{nm}(z,t)$ is the slowly varying amplitude of the corresponding electric field component. For the nonlinear fibers

considered here, we assume that the magnitude and orientation of the birefringence is uniform throughout the length of the fiber, and we have chosen to orient the x- and y-axes to point along the birefringence directions.

If we assume that the pump ($n = 1$) is much stronger than the probe signal ($n = 2$), the probe's slowly-varying amplitudes A_{2x} and A_{2y} are governed by the coupled nonlinear equations [30], given by

$$\begin{aligned}\frac{\partial A_{2x}}{\partial z} + \beta'_{2x}\frac{\partial A_{2x}}{\partial t} + \frac{i}{2}\beta''_{2x}\frac{\partial^2 A_{2x}}{\partial t^2} &= i\gamma\left(2|A_{1x}|^2 + \frac{2}{3}|A_{1y}|^2\right)A_{2x} \\ &+ \frac{2i\gamma}{3}A^*_{1x}A_{1y}A_{2y}e^{i[(\beta_{1y}-\beta_{1x})+(\beta_{2y}-\beta_{2x})]z} \\ &+ \frac{2i\gamma}{3}A_{1x}A^*_{1y}A_{2y}e^{-i[(\beta_{1y}-\beta_{1x})-(\beta_{2y}-\beta_{2x})]z} \qquad (2a)\end{aligned}$$

$$\begin{aligned}\frac{\partial A_{2y}}{\partial z} + \beta'_{2y}\frac{\partial A_{2y}}{\partial t} + \frac{i}{2}\beta''_{2y}\frac{\partial^2 A_{2y}}{\partial t^2} &= i\gamma\left(2|A_{1y}|^2 + \frac{2}{3}|A_{1x}|^2\right)A_{2y} \\ &+ \frac{2i\gamma}{3}A^*_{1y}A_{1x}A_{2x}e^{i[(\beta_{1x}-\beta_{1y})+(\beta_{2x}-\beta_{2y})]z} \\ &+ \frac{2i\gamma}{3}A_{1y}A^*_{1x}A_{2x}e^{-i[(\beta_{1x}-\beta_{1y})-(\beta_{2x}-\beta_{2y})]z} \qquad (2b)\end{aligned}$$

where β'_{nm} and β''_{nm} are the first and second derivatives of the propagation constant evaluated at the nth carrier frequency. For example, β''_{1x} is defined as

$$\beta''_{1x} = \left.\frac{\partial^2 \beta_x(\omega)}{\partial \omega^2}\right|_{\omega=\omega_1}. \qquad (3)$$

If the pump is linearly polarized along one of the fiber axes, then (2a) and (2b) predict that the cross-phase modulation will be $3\times$ stronger for the copolarized component of the probe signal than for the cross-polarized component, leading to unacceptable polarization dependence.

In the special case that the fiber birefringence is zero, i.e., $\beta_x(\omega) = \beta_y(\omega)$, the coupled equations can be simplified to

$$\begin{aligned}\frac{\partial A_{2x}}{\partial z} + \beta'\frac{\partial A_{2x}}{\partial t} + \frac{i}{2}\beta''\frac{\partial^2 A_{2x}}{\partial t^2} &= i\gamma\left(2|A_{1x}|^2 + \frac{2}{3}|A_{1y}|^2\right)A_{2x} \\ &+ \frac{2i\gamma}{3}\left(A^*_{1x}A_{1y} + A_{1x}A^*_{1y}\right)A_{2y} \qquad (4a)\end{aligned}$$

$$\begin{aligned}\frac{\partial A_{2y}}{\partial z} + \beta'\frac{\partial A_{2y}}{\partial t} + \frac{i}{2}\beta''\frac{\partial^2 A_{2y}}{\partial t^2} &= i\gamma\left(2|A_{1y}|^2 + \frac{2}{3}|A_{1x}|^2\right)A_{2y} \\ &+ \frac{2i\gamma}{3}\left(A^*_{1y}A_{1x} + A_{1y}A^*_{1x}\right)A_{2x}. \qquad (4b)\end{aligned}$$

If the pump remains circularly polarized, i.e., $A_{2y} = \pm iA_{2x}$, then the last terms on the right-hand sides of (4a) and (4b) vanish, yielding identical decoupled equations describing the evolution of A_{2x} and A_{2y}. In this case, the process of cross-phase modulation will not depend on the polarization state of the probe signal. Unfortunately, when the fiber exhibits linear birefringence, it is impossible for the polarization state to remain circular as the signal propagates.

In the following two sections, we describe two techniques that can be used to achieve polarization-independent cross-phase modulation, even in cases when the nonlinear fiber has linear birefringence.

IV. Method I: High Differential Group Delay

In a linearly birefringent fiber, there is no way to maintain the circular polarization state for the pump signal. As a result of the linear birefringence, any input polarization state that is not aligned with one of the birefringence axes will periodically change with distance as it propagates along the fiber. The period of this evolution is known as the beat length, described by

$$L_b = \frac{2\pi}{|\beta_x - \beta_y|} \qquad (5)$$

where β_x and β_y describe the propagation constants of the x- and y-polarized modes. In general, because the pump and probe signals have different wavelengths, they will also have different beat lengths. We show here that, if the difference between the beat lengths is large enough, polarization-independent cross-phase modulation can be achieved.

A. Theory

Consider the last two terms appearing on the right-hand side of (2a). Most birefringent fibers are significantly longer than the beat length, which implies that the first of these oscillating terms can be neglected since the exponential term completes many cycles within the length of the fiber. The argument of the last exponential term on the right-hand side of (2a) contains the difference $[(\beta_{1y} - \beta_{1x}) - (\beta_{2y} - \beta_{2x})]$. This term can also average to zero, provided the following condition holds:

$$|(\beta_{1y} - \beta_{1x}) - (\beta_{2y} - \beta_{2x})|\, L \gg 2\pi. \qquad (6)$$

The difference between the propagation constants can be approximated as $\beta_{1x} - \beta_{2x} \simeq \beta'_{1x}\Delta\omega$, where β'_{1x} is the inverse group velocity for signals polarized along the x-direction. Using this relation, the condition described in (6) can be expressed in terms of the total fiber differential group delay (DGD), $\Delta\tau \equiv (\beta'_{1x} - \beta'_{1y})L$, and the frequency separation between pump and probe $\Delta\omega$:

$$\Delta\omega\Delta\tau \gg 2\pi. \qquad (7)$$

Note that, in our analysis, we consider the case where the net DGD of the fiber is small compared with the optical pulsewidths. We can, therefore, eliminate those terms that include the first derivative with respect to time in (2a) and (2b) by changing to a reference frame moving with the mean group velocity. We also assume that $\beta''_{2x} \approx \beta''_{2y} \equiv \beta''$. After simplifying the equations

using these assumptions, we obtain

$$\frac{\partial A_{2x}}{\partial z} + \frac{i}{2}\beta''\frac{\partial^2 A_{2x}}{\partial \tau^2} \simeq i\gamma\left(2|A_{1x}|^2 + \frac{2}{3}|A_{1y}|^2\right)A_{2x} \quad (8a)$$

$$\frac{\partial A_{2y}}{\partial z} + \frac{i}{2}\beta''\frac{\partial^2 A_{2y}}{\partial \tau^2} \simeq i\gamma\left(2|A_{1y}|^2 + \frac{2}{3}|A_{1x}|^2\right)A_{2y} \quad (8b)$$

where $\tau \equiv t - \bar{\beta}'z$ is the retarded time measured in the moving reference frame and $\bar{\beta}'$ is the mean of β'_{2x} and β'_{2y}. It can be seen that, if $|A_{1x}|^2 = |A_{1y}|^2$, that is, if the pump signal is polarized so that it equally excites both principal axes, (8a) and (8b) become identical. The cross-phase modulation process will, therefore, be polarization independent under these conditions. A similar argument can be used to predict polarization independence in optical parametric amplifiers [31].

The wavelength separation between the pump and probe signals is an important parameter that determines the polarization dependence of the cross-phase modulation process, as described by (7). To better quantify this effect, we now consider the solution to (2a) and (2b) when the last oscillating term is retained, i.e., when (7) does not hold. We assume that the pump signal has an instantaneous power of $P(\tau)$ and is polarized so that it equally excites the principal axes of the fiber. Neglecting pump depletion and dispersion, this gives

$$|A_{1x}(z,\tau)| = |A_{1y}(z,\tau)| = \sqrt{\frac{P(\tau)}{2}}. \quad (9)$$

Under these assumptions, the coupled equations for A_{2x} and A_{2y} become

$$\frac{\partial A_{2x}}{\partial z} = i\frac{4\gamma P(\tau)}{3}\left[A_{2x}(z,\tau) + \frac{e^{+i\kappa z}}{4}A_{2y}(z,\tau)\right] \quad (10a)$$

$$\frac{\partial A_{2y}}{\partial z} = i\frac{4\gamma P(\tau)}{3}\left[A_{2y}(z,\tau) + \frac{e^{-i\kappa z}}{4}A_{2x}(z,\tau)\right] \quad (10b)$$

where $\kappa \equiv (\beta_{1y} - \beta_{1x}) - (\beta_{2y} - \beta_{2x})$.

To simplify the analysis, we consider the case that the probe signal is initially a continuous-wave (CW) signal with an arbitrary state of polarization

$$A_{2x}(0,\tau) = u_x, \quad A_{2y}(0,\tau) = u_y \quad (11)$$

where u_x and u_y are complex constants describing the Jones vector of the input CW signal.

The solution for $A_{2x}(z,\tau)$ and $A_{2y}(z,\tau)$ can be obtained by direct integration of (10a) and (10b). In the limit that $\gamma P(\tau)L$ is small, the solution may be approximated as

$$A_{2x}(L,\tau) \simeq u_x + i\frac{\gamma P(\tau)L}{3}\left[4u_x + e^{+i\kappa L/2}\frac{\sin(\kappa L/2)}{\kappa L/2}u_y\right] \quad (12a)$$

$$A_{2y}(L,\tau) \simeq u_y + i\frac{\gamma P(\tau)L}{3}\left[4u_y + e^{-i\kappa L/2}\frac{\sin(\kappa L/2)}{\kappa L/2}u_x\right]. \quad (12b)$$

The optical spectrum of the cross-phase-modulated tone can be found by computing the Fourier transforms of (12a) and (12b), and summing their intensities. The leading terms appearing in (12a) and (12b) correspond to the CW tone emerging from the fiber, while the additional time-varying terms describe a spectral pedestal surrounding the CW tone, as depicted in Fig. 3. The shape of this spectral pedestal will be proportional to the Fourier transform of the pump signal $P(t)$, but its intensity will depend upon the polarization state of the input signal, described by u_x and u_y, and the product $\kappa L \equiv \Delta\omega\,\Delta\tau$.

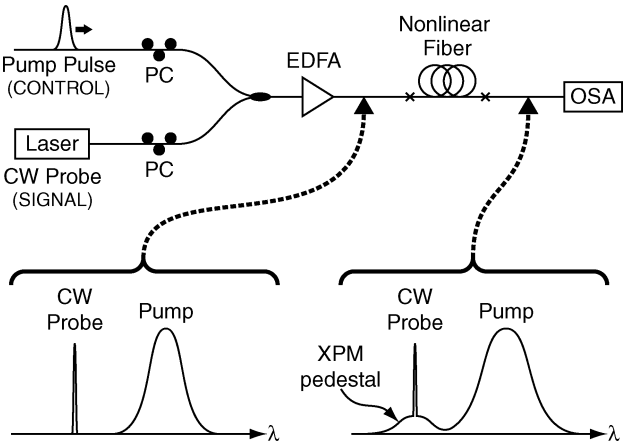

Fig. 3. Experimental setup used to study cross-phase modulation of a continuous-wave probe signal by an intense Gaussian pulse. Through cross-phase modulation, the strong pulse induces a broad spectral pedestal on the CW signal that is observed on a spectrum analyzer as a function of the input polarization states.

When the product κL is large, the terms involving $\sin(\kappa L/2)/(\kappa L/2)$ can be neglected, and the output signals A_{2x} and A_{2y} are seen to be directly proportional to u_x and u_y, respectively. This condition results in an output power spectrum that depends only on the input signal power $|u_x|^2 + |u_y|^2$, but not on its polarization state. Similar polarization independent behavior is expected whenever $\kappa L = 2\pi m$, where m is an integer.

B. Experimental Measurements and Numerical Simulation

Fig. 3 depicts the experimental setup used to study the polarization dependence of cross-phase modulation. A strong pump pulse from a mode-locked fiber laser was combined with a CW tone, amplified and injected into the nonlinear fiber. We then measured the output spectrum of the cross-phase-modulated CW tone as a function of the input polarization state and the wavelength separation between the pump and probe.

In order to enable sufficiently high values of $\Delta\omega\,\Delta\tau$, we used the 30 m photonic crystal fiber described in Table I, with pump and signal wavelengths adjusted to 1542 and 1551.9 nm, respectively, which gives $\Delta\omega\,\Delta\tau = 10$. The pump pulsewidth was 2.5 ps, the repetition rate was 10 GHz, and the average powers of the pump and probe entering the nonlinear fiber were 21 and 13 dBm, respectively. As depicted in the lower portion of Fig. 3, cross-phase modulation produces a broad spectral pedestal around the CW tone, which was observed to rise and fall depending on the polarization states of the pump and probe.

Fig. 4(a) and (b) plots the experimentally measured spectra of the CW tone, after propagating through the nonlinear fiber

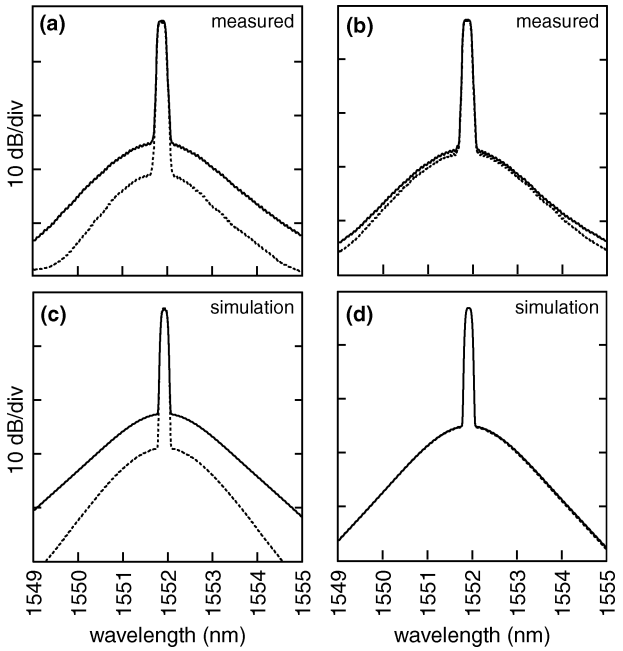

Fig. 4. (a) Experimentally measured minimum and maximum cross-phase-modulation pedestals obtained by adjusting the CW signal polarization state, showing up to 8 dB of polarization dependence. During these measurements, the pump polarization was held constant at the setting that produced the greatest polarization dependence. (b) Same measurements, but taken with the pump polarization experimentally adjusted to yield the smallest polarization dependence. (c) Numerical simulation of the cross-phase modulation pedestal assuming that the pump is linearly polarized along one of the fiber axes. (d) Numerical simulation of the cross-phase modulation pedestal for the case when the pump is polarized to equally excite the fiber axes.

with the strong pump pulse (not depicted). In both cases, we plot the measured minimum and maximum spectra obtained by varying the probe polarization state, while holding the pump polarization state constant. The corresponding simulated spectra plotted in Fig. 4(c) and (d) were numerically computed using a vector split-step method, based on the measured fiber properties and optical signal parameters.

For the data shown in Fig. 4(a), we experimentally adjusted the pump polarization in order to yield the maximum dependence on the probe polarization ($\sim$8 dB). Although it is difficult to accurately measure the input pump polarization state and fiber orientation, the corresponding numerical simulation shown in Fig. 4(c) was performed assuming that the pump was linearly polarized along one of the fiber axes, and shows excellent agreement with the measurements. The simulation furthermore confirmed that the strongest cross-phase modulation pedestal results when the pump and probe are copolarized while the weakest cross-phase modulation pedestal occurs when they are cross-polarized, all other cases falling between these extremes.

Conversely, when the pump polarization was optimally adjusted, we observed that the polarization dependence was almost eliminated over the entire cross-phase modulation pedestal, as shown in Fig. 4(b). This case is well matched by the numerical simulations shown in Fig. 4(d), in which the pump polarization was chosen to equally excite the axes of the fiber.

In order to investigate how the polarization dependence relates to the frequency separation $\Delta\omega$, we tuned the wavelength of

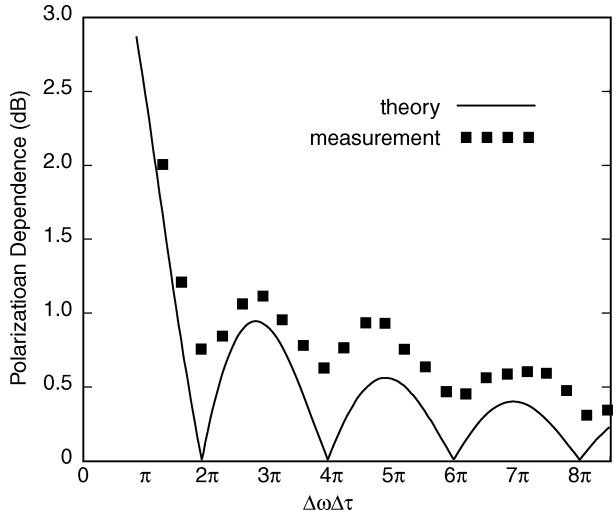

Fig. 5. Measured and theoretically predicted polarization dependence of cross-phase modulation as a function of $\Delta\omega\Delta\tau$.

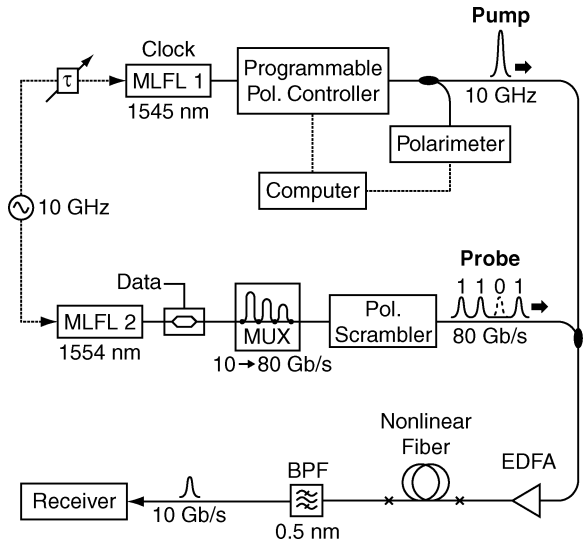

Fig. 6. Diagram of optical demultiplexing experiment using cross-phase modulation. To evaluate the polarization sensitivity, the data polarization was continuously scrambled while observing the bit-error-rate and eye diagram at the receiver.

the probe signal while leaving the pump polarization adjusted to the optimal state. Fig. 5 plots the experimentally observed polarization dependence (in decibels) as a function of the dimensionless quantity $\Delta\omega\,\Delta\tau$. The solid line plots the polarization dependence calculated analytically from (12a) and (12b), showing agreement with the experimental data. For these measurements, the wavelength separation between pump and probe was varied from 4 to 26 nm, corresponding to a $\Delta\omega$ of 3×10^{12} to 2×10^{13} rad/s, and the $\Delta\tau$ used for the PCF was 1.26 ps, as given in Table I. It is seen that to reduce the polarization dependence to <1 dB, it is only required to have $\Delta\omega\Delta\tau > 2\pi$.

Finally, we utilized this technique to demonstrate polarization-independent all-optical demultiplexing of an 80 Gb/s data channel [32]. For this measurement, the CW probe was replaced with an 80 Gb/s data signal, which was produced from a second 10 GHz mode-locked fiber laser, as shown in Fig. 6.

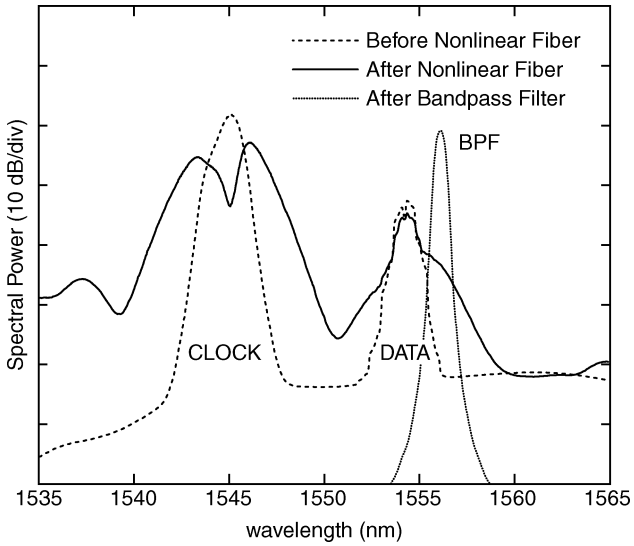

Fig. 7. Optical spectra for the 80 Gb/s demultiplexing experiment measured before the highly nonlinear photonic crystal fiber (dashed), after the nonlinear fiber (solid), and after spectral filtering (dotted) [32].

The signal was modulated with a 10 Gb/s, $2^7 - 1$ pseudorandom bit sequence (PRBS), and passively multiplexed to 80 Gb/s. The relative delay between the clock and data pulses was electronically adjusted in order to selectively red-shift one of the eight tributary channels. The data polarization state was randomly scrambled at a rate of 1 MHz, in order to obtain the worst case impairment from polarization dependence. Meanwhile, the clock polarization was controlled via computer and measured by a polarimeter in order to ascertain which clock polarizations gave the best performance.

Fig. 7 plots the optical spectrum of the clock and data measured before the nonlinear fiber, after the nonlinear fiber, and after the bandpass filter. The data signal was detuned by 9 nm relative to the pump wavelength in order to satisfy (7), and the bandpass filter was detuned by 2 nm relative to the data wavelength in order to isolate the red-shifted tributary. In practice, the wavelength separation cannot be made arbitrarily large because eventually chromatic dispersion would cause the pump and probe signals to walk off, limiting the effective length of the interaction. For the low-dispersion PCF considered here, even when the wavelengths were separated by almost 10 nm, the temporal walk off caused by chromatic dispersion between the pump and probe wavelengths was only 135 fs, which was significantly smaller than both the pulse widths and polarization DGD.

Fig. 8 plots the eye diagrams of the demultiplexed data measured after the bandpass filter. In Fig. 8(a), the clock was polarized along one of the fiber axes, in which case the cross-phase modulation efficiency can vary by up to 8 dB depending on the data polarization state [cf., Fig. 4(a)]. Because the data polarization is scrambled, the resulting eye diagram is completely closed, leading to a bit error rate (BER) exceeding 10^{-2}. By contrast, in Fig. 8(b), the clock was polarized in a way that equally excites both fiber axes. In this case, we achieve an open

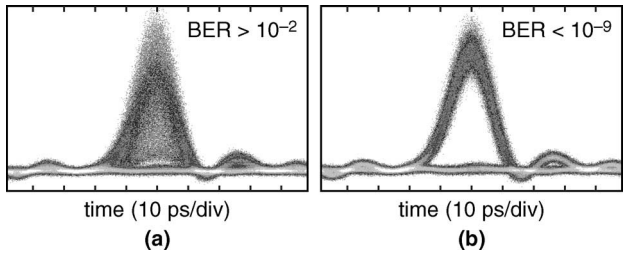

Fig. 8. Observed eye diagram of demultiplexed data (a) When the pump polarization is chosen incorrectly. (b) For the optimal pump polarization state.

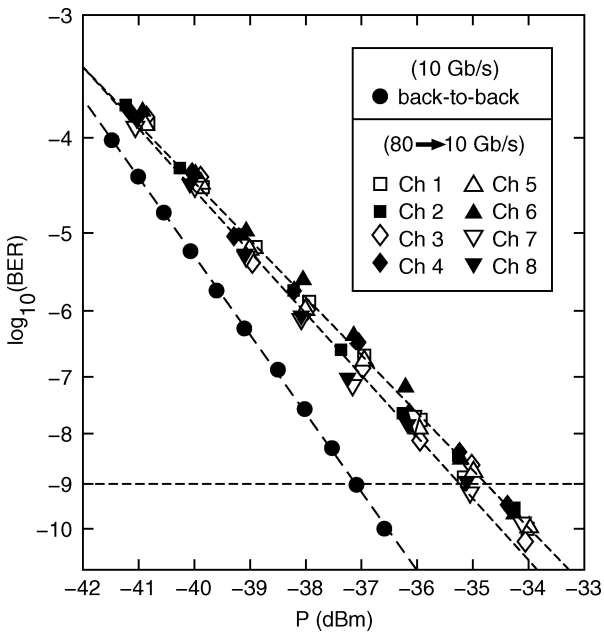

Fig. 9. Measured BER versus the received optical power for the eight tributaries that were temporally demultiplexed from an aggregate 80 Gb/s stream. In all cases, the data signal was polarization-scrambled prior to cross-phase modulation, in order to simulate the worst case polarization impairment [32].

eye diagram, and error-free performance, even while the data polarization is randomly scrambled [32].

Fig. 9 plots the measured BER performance for the eight demultiplexed channels, in comparison to a back-to-back baseline measurement at 10 Gb/s. During the demultiplexing measurements, the polarization state of the data signal was continuously scrambled while recording the BER. Despite the polarization scrambling, all channels achieve error-free performance, with no sign of an error floor, indicating that polarization dependence has been effectively suppressed.

The theory described in Section IV-A predicts that polarization-independent demultiplexing will occur for any clock polarization that equally excites both fiber axes (provided $\Delta\omega\,\Delta\tau \gg 2\pi$). The range of optimal clock polarization states should, therefore, describe a great circle on the Poincaré sphere. To test this theory, the clock polarization was systematically set to 1000 different states distributed uniformly over the Poincaré sphere, while at each point, the BER of the demultiplexed signal was measured. In all measurements, the data polarization was randomly scrambled in order to produce the worst-case

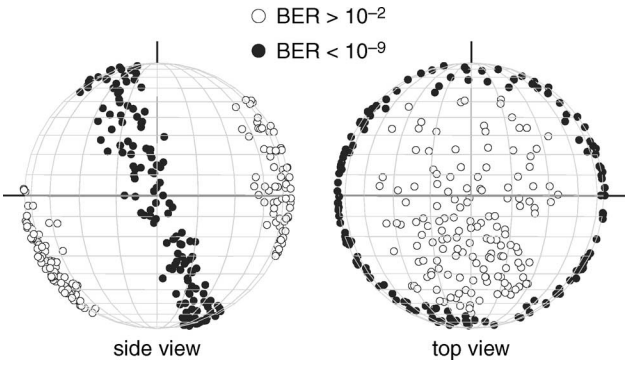

Fig. 10. Measured BER as a function of pump polarization state on the Poincaré sphere. This picture shows that the optimal pump polarization states (i.e., those that produce a low BER) all lie on a great circle on the Poincaré sphere. This observation supports the theory that polarization-independent behavior results when the the fiber eigenstates are equally excited.

polarization penalty. The filled circles plotted in Fig. 10 indicate the clock polarization states for which the demultiplexed data achieved a BER better than 10^{-9}, whereas the open circles indicate the clock polarizations for which the BER rose above 3×10^{-2}. Because we do not know the Jones matrix of the intervening fiber between the polarimeter and the nonlinear fiber, it is impossible to map the measurements shown in Fig. 10 into the exact polarization state entering the nonlinear fiber. Nonetheless, these results clearly show that the maximum polarization dependence (high BER) is obtained for two orthogonal polarization states, which we infer must correspond to the eigenstates of the fiber. Minimal polarization dependence (low BER) is obtained for a circle of polarization states lying between these two orthogonal axes, in agreement with theory.

This technique should not be limited to the PCF class of fibers, but for the method to work, several key parameters must be controlled. While a higher DGD relaxes the requirement on the wavelength separation between pump and probe, it may be incompatible with the desired data rate. Lowering the DGD increases the required separation, in which case the pulse walk-off due to chromatic dispersion must be considered, as with any fiber-based nonlinear device. Furthermore, while here we have focused on utilizing the spectral shift resulting from X pixmal (XPM), as was used in the first published experiments [32], we note that this technique has since been applied to demonstrations of polarization-independent four-wave mixing [33], [34]. We also expect, based on the theoretical results, that this method should be applicable to interferometric devices based directly on the XPM-induced phase shift, although further research is needed in this area.

V. Method II: Spectral Crossing

In the previous section, we demonstrated that the spectral density generated by the cross-phase modulation can be made polarization independent, provided the fiber birefringence and wavelength separation satisfy (7). In some nonlinear fibers, it is difficult to achieve this condition, either because the birefringence is too low, or the fiber is too short. For example, in a 2-m-long bismuth-oxide-based fiber with parameters given in Table I, the wavelength separation between the pump and the probe would have to be about 120 nm in order to satisfy (7).

In many applications, including wavelength conversion and demultiplexing, we need the cross-phase modulation spectral density to be polarization-independent only within a small bandwidth corresponding to bandpass filter. We now explain how a polarization-independent wavelength can be found in the cross-phase modulation-generated spectrum. By tuning the bandpass filter to this wavelength, optical switching with very low polarization sensitivity can be achieved.

A. Theory

To begin, we assume that the pump is initially polarized along the x-axis of the fiber. If the fiber axes are uniformly oriented over its length, then the pump will remain linearly polarized throughout the fiber, allowing us to conclude that $A_{1y} = 0$. In this case, (2a) and (2b) simplify to

$$\frac{\partial A_{2x}}{\partial z} + \beta'_{2x}\frac{\partial A_{2x}}{\partial t} + \frac{i}{2}\beta''_{2x}\frac{\partial^2 A_{2x}}{\partial t^2} = i\gamma 2|A_{1x}|^2 A_{2x} \quad (13a)$$

$$\frac{\partial A_{2y}}{\partial z} + \beta'_{2y}\frac{\partial A_{2y}}{\partial t} + \frac{i}{2}\beta''_{2y}\frac{\partial^2 A_{2y}}{\partial t^2} = i\gamma\frac{2}{3}|A_{1x}|^2 A_{2y}. \quad (13b)$$

Once the pump evolution $A_{1x}(z,t)$ is determined, (13a) describes a linear, time-varying system relating the input probe signal $A_{2x}(0,t)$ to the output $A_{2x}(L,t)$. The system is linear because all terms in the governing differential equations are linearly related to the probe amplitude A_{2x}, but time-varying because the proportionality constant appearing on the right-hand side depends on t through $|A_{1x}(z,t)|^2$. Equation (13b) is likewise a linear time-varying system that can be integrated to find the output $A_{2y}(L,t)$ from the input $A_{2y}(0,t)$.

We now suppose that the input probe signal has intensity $p(t)$ and is polarized in the x-direction. Because (13a) and (13b) are decoupled, the output signal must also be polarized in the x-direction. In general, we could express the solution as

$$A_{2x}(L,t) = h_x(t), \qquad A_{2y}(L,t) = 0 \quad (14)$$

where the function $h_x(t)$ is obtained by solving (13a) under the assumption that $A_{2x}(0,t) = \sqrt{p(t)}$.

If the input signal had the same intensity, but were instead polarized in the y-direction, then the output could, in general, be represented as

$$A_{2x}(L,t) = 0, \qquad A_{2y}(L,t) = h_y(t) \quad (15)$$

where the function $h_y(t)$ is similarly obtained by integrating (13b) with the initial condition that $A_{2y}(0,t) = \sqrt{p(t)}$.

We now suppose that the input probe signal has an intensity $p(t)$ and an arbitrary polarization state

$$\begin{bmatrix} A_{2x}(0,t) \\ A_{2y}(0,t) \end{bmatrix} = \sqrt{p(t)}\begin{bmatrix} e_x \\ e_y \end{bmatrix} \quad (16)$$

where e_x and e_y are complex numbers specifying the Jones vector of the input signal, normalized so that $|e_x|^2 + |e_y|^2 = 1$. Because (13a) and (13b) are linear, we conclude that the output signal is given by a superposition of (14) and (15):

$$A_{2x}(L,t) = e_x h_x(t), \qquad A_{2y}(L,t) = e_y h_y(t). \quad (17)$$

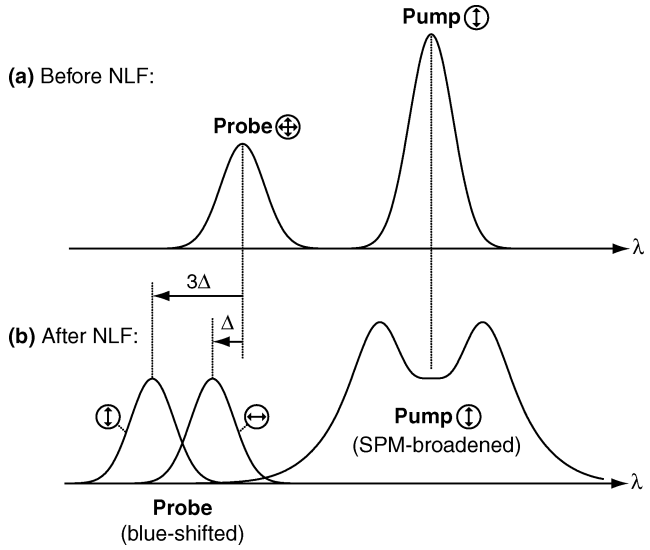

Fig. 11. Illustration of how the spectral shift produced through cross-phase modulation depends upon the relative polarization state of the pump and probe. The greatest shift is produced when the pump and probe are copolarized, while the spectral shift is 3× smaller when the pump and probe are cross-polarized.

The output power spectrum of the probe signal is then given by

$$S(\omega) = |e_x|^2 |H_x(\omega)|^2 + |e_y|^2 |H_y(\omega)|^2 \tag{18}$$

where $H_j(\omega)$ denotes the Fourier transform of the time signal $h_j(t)$ (where $j = x, y$).

Finally, suppose that the functions $|H_x(\omega)|^2$ and $|H_y(\omega)|^2$ were to intersect at some frequency ω_0, i.e,

$$|H_x(\omega_0)|^2 = |H_y(\omega_0)|^2 \equiv S_0. \tag{19}$$

At this frequency, the output spectral density is given by

$$S(\omega_0) = S_0(|e_x|^2 + |e_y|^2) = S_0 \tag{20}$$

which does not depend on the input polarization state. This result, which is based entirely on the linearity of the differential equations, and makes no assumptions about the dispersion, loss, or birefringence, proves that if the output cross-phase modulation spectra intersect for two different input polarizations, then they must intersect for all possible input polarizations. We next address the question of how to ensure that such a crossing point exists.

In an earlier work, we explained how such a spectral crossing point can be achieved with a CW probe signal [35]. Here, we consider the more interesting and practical case when both the pump and probe are optical pulses, temporally aligned so as to induce a spectral shift of the weaker probe pulse, as depicted in Fig. 1. By comparing the right-hand sides of (13a) and (13b), we expect that when the signal is copolarized with the pump, the cross-phase modulation-induced spectral shift will be 3× larger than in the cross-polarized case. As depicted schematically in Fig. 11, we, therefore, expect that the two output spectra will exhibit an intersection point. The theory presented before predicts that any intermediate polarization state will yield a cross-phase modulation spectrum that reaches the same intersection point.

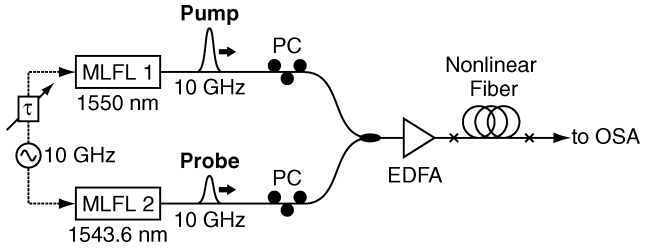

Fig. 12. Experimental setup used to observe the polarization dependence of cross-phase modulation between two optical pulses.

The position of the spectral crossing point is proportional to the pump power. In practice, the pump power must be sufficiently large to allow the spectrally shifted channel to be separated from the remaining channels with a bandpass filter.

If the pump signal is not polarized along one of the principle axes of the fiber, the role of the nonlinear polarization rotation should be considered when determining the pump evolution [36]. In this case the x-polarized and y-polarized input probes generate outputs that have both x-and y-components. As long as the outputs corresponding to x-and y-polarized inputs remain orthogonal, the same argument can be used to predict that any crossing point in the output spectra will be polarization-independent. Our experimental measurements and numerical simulations show that the polarization-independent point can be found for any pump polarization state.

B. Experimental Measurements and Numerical Simulation

Fig. 12 depicts the experimental setup used to observe the polarization-independent crossing point in the cross-phase modulation spectrum. The pump and probe pulses were generated by two synchronized 10 GHz mode-locked fiber lasers, with wavelengths of 1550 and 1534.6 nm and pulsewidths of 1.8 and 2.5 ps, respectively. The pump and the probe were amplified to an average power of 22.5 and 12.5 dBm, respectively, and launched into 2 m of highly nonlinear bismuth-oxide-based fiber, with parameters given in Table I. The relative delay between the pump and the probe was adjusted to produce a blue-shift of the probe pulses.

Fig. 13(a) plots the experimentally measured optical spectra before and after the nonlinear fiber. The two solid curves show the minimum and maximum spectral shift that could be obtained by adjusting the probe polarization state. Although it is impossible to precisely quantify the input polarization states corresponding to these spectra, it is notable that the spectral shift varies by a factor of approximately 3×, as expected. More significantly, the measured spectra for all other polarization states were observed to fall between the two extreme cases plotted here.

Fig. 13(b) shows the results of a numerical simulation, calculated using a full-vector split-step propagation solver. The simulation used only the measured optical and material properties, with no adjustable fitting parameters. The output spectra were calculated for 16 different input probe polarization states distributed evenly on the Poincaré sphere.

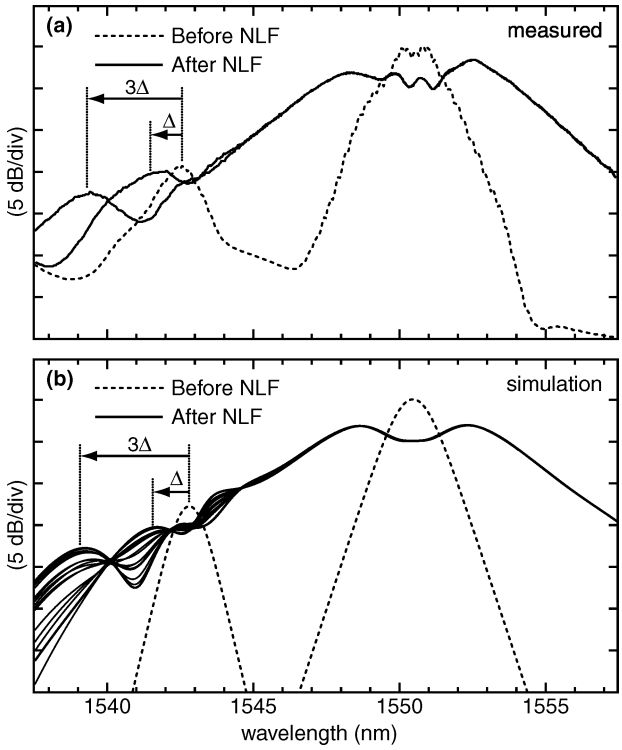

Fig. 13. (a) Measured optical spectrum of pump and probe pulse after cross-phase modulation, showing the minimum and maximum spectral shift. (b) Numerically calculated optical spectra for the minimum and maximum case, as well as 14 other polarization states distributed around the Poincaré sphere.

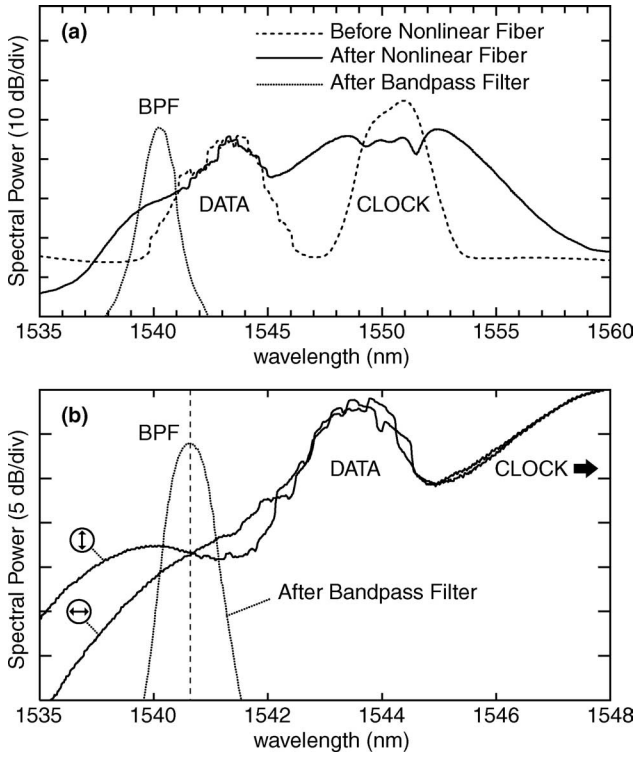

Fig. 14. (a) Observed optical spectra for 160 Gb/s optical demultiplexing experiment before the HNLF (dashed), after the HNLF (solid) and after the BPF (dotted). (b) Enlarged view of the cross-phase modulation spectrum of the data signal for two extreme polarization states, showing the distinct crossing point and the location of the output spectral filter [35].

The simulations show excellent agreement with the measurements, confirming that all of the spectra intersect at the same point. We note that the spectrum measurements were performed with an instrument resolution bandwidth of 0.5 nm, which was also incorporated in the simulation. Thus, even when the spectra are viewed through an 0.5 nm bandpass filter, they exhibit a distinct crossing point. Polarization-independent cross-phase modulation can, therefore, be achieved by adjusting the output bandpass filter to coincide with a crossing point in the optical spectrum.

As with the first method, we applied this technique to demonstrate high-speed all-optical switching, using a setup similar to that depicted in Fig. 6. In this experiment, the 10 GHz probe signal was modulated with a $2^{23} - 1$ pseudorandom data sequence and passively multiplexed to 160 Gb/s. The average powers of the clock and data before entering the nonlinear fiber were 22.5 and 12.5 dBm, respectively. Fig. 14(a) plots the optical spectra measured before the nonlinear fiber, after the nonlinear fiber, and after the bandpass filter, for one specific input polarization state. Fig. 14(b) shows an enlarged plot of the cross-phase-modulated data, showing the minimum and maximum spectra obtained by varying the data polarization state. The bandpass filter is tuned to the the intersection point of the spectra, at which point we expect polarization-independent behavior.

In order to evaluate the system performance in the presence of polarization fluctuations, a high-speed polarization scrambler was inserted in the data path. Fig. 15(a) plots the demultiplexed eye diagram (10 Gb/s) when the spectral filter was misaligned,

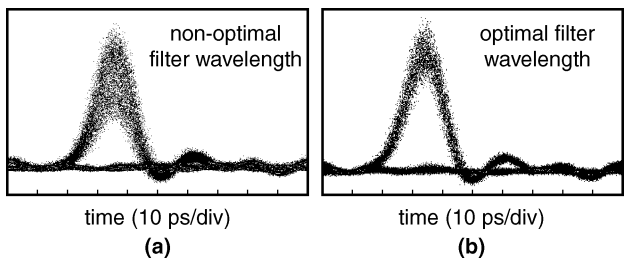

Fig. 15. Observed eye diagram of demultiplexed data. (a) Non-optimal filter tuning. (b) With the pump power and spectral filter chosen optimally.

resulting in a significant eye closure associated with polarization dependence. The clock power and bandpass filter wavelength were then adjusted while monitoring the BER and eye diagram in order to achieve the lowest degree of polarization dependence. Fig. 15(b) plots the resulting open eye diagram when the filter is optimally tuned. Fig. 16 plots the measured BER as a function of the received power for the 10 Gb/s demultiplexed channel, in comparison to a back-to-back 10 Gb/s measurement. The BER curves measured with the polarization scrambler enabled are indistinguishable from the curves measured with a static polarization state, thus confirming polarization-independent performance.

In addition to the demultiplexing experiments reviewed here, this technique has recently been used for all-optical retiming using XPM and spectral slicing in a length of standard highly

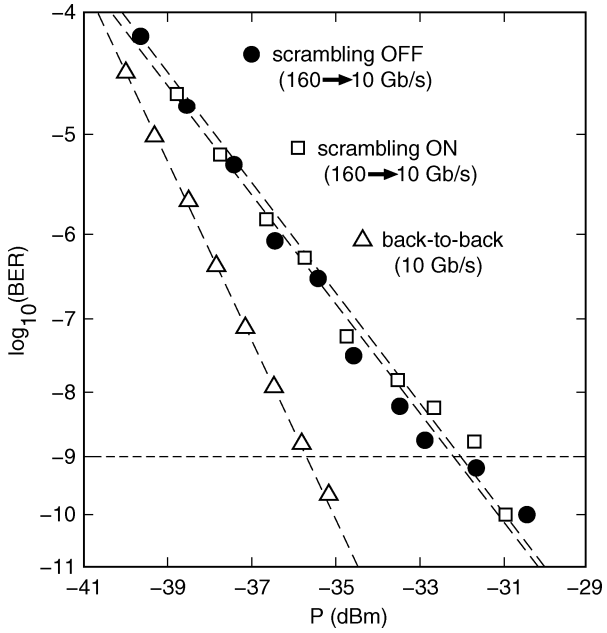

Fig. 16. Measured bit error rate vs. received optical power. The baseline curve represents a back-to-back measurement at 10 Gb/s with no optical demultiplexing. The other two curves plot the performance of the 160–10 Gb/s demultiplexing system when the input polarization is static and when the input polarization is randomly scrambled, showing that there is no significant error penalty incurred as a result of polarization scrambling [35].

nonlinear fiber [37]. This technique should also be applicable to other devices based on XPM and spectral filtering. For example, the CW probe results presented in [35] could be easily adapted to XPM-based wavelength conversion [38], although for high data rates, optimizing the filtering for the dual requirements of polarization independence and short pulsewidths will necessitate further research. It is perhaps less applicable to schemes such as nonlinear interferometers based directly on the XPM-induced phase shift; however, a thorough investigation of this issue has not been undertaken, and is beyond the scope of the present paper.

VI. Conclusion

The polarization dependence of nonlinear optical processes remains an important problem that limits the practicality of many all-optical switches. Although techniques have been proposed to overcome this polarization dependence, most require significant changes to the experimental apparatus. We here describe two different methods to achieve polarization-independent cross-phase modulation that do not significantly complicate the experimental setup. Using these techniques, we demonstrate error-free all-optical demultiplexing at speeds of up to 160 Gb/s, even when the input polarization is randomly scrambled.

One important enabling technology behind these results is the development of highly nonlinear fibers that can yield a sufficient nonlinearity in a just few meters of fiber. Because of their short lengths, it is possible to control the polarization evolution in these fibers in ways that were simply impossible in kilometer-length fibers. Although most nonlinear fibers are designed to be nonbirefringent, unintentional asymmetries in the fabrication process often lead to significant linear birefringence. The results reported here suggest that a small, controllable birefringence in nonlinear fibers could be exploited to achieve polarization-independent all-optical switching.

Acknowledgment

The authors thank N. Sugimoto of Asahi Glass Company, Ltd, for providing the Bi_2O_3-based fiber used in this paper.

References

[1] N. J. Doran and D. Wood, "Nonlinear-optical loop mirror," *Opt. Lett.*, vol. 13, no. 1, pp. 56–58, 1988.

[2] M. N. Islam, E. R. Sunderman, R. H. Stolen, W. Pleibel, and J. R. Simpson, "Soliton switching in a fiber nonlinear loop mirror," *Opt. Lett.*, vol. 14, no. 15, pp. 811–813, 1989.

[3] B.-E. Olsson and D. J. Blumenthal, "All-optical demultiplexing using fiber cross-phase modulation (XPM) and optical filtering," *IEEE Photon. Technol. Lett.*, vol. 13, no. 8, pp. 875–877, Aug. 2001.

[4] J. Li, B.-E. Olsson, M. Karlsson, and P. A. Andrekson, "OTDM demultiplexer based on XPM-induced wavelength shifting in highly nonlinear fiber," *IEEE Photon. Technol. Lett.*, vol. 15, no. 12, pp. 1770–1772, Dec. 2003.

[5] J. H. Lee, T. Tanemura, K. Kikuchi, T. Nagashima, T. Hasegawa, S. Ohara, and N. Sugimoto, "Use of 1-m Bi_2O_3 nonlinear fiber for 160-Gbit/s optical time-division demultiplexing based on polarization rotation and a wavelength shift induced by cross-phase modulation," *Opt. Lett.*, vol. 30, no. 11, pp. 1267–1269, 2005.

[6] J. Yu and P. Jeppesen, "80-Gb/s Wavelength conversion based on cross-phase modulation in high-nonlinearity dispersion-shifted fiber and optical filtering," *IEEE Photon. Technol. Lett.*, vol. 13, no. 8, pp. 833–835, Aug. 2001.

[7] V. Perlin and H. G. Winful, "All-fiber wavelength conversion using cross-phase modulation and Bragg Gratings," *IEEE Photon. Technol. Lett.*, vol. 14, no. 2, pp. 176–178, Feb. 2002.

[8] A. Bogoni, P. Ghelfi, M. Scaffardi, and L. Poti, "All-optical regeneration and demultiplexing for 160-Gb/s transmission systems using a NOLM-based three-stage scheme," *J. Quantum Electron.*, vol. 10, no. 1, pp. 192–196, 2004.

[9] J. Suzuki, T. Tanemura, K. Taira, Y. Ozeki, and K. Kikuchi, "All-optical regenerator using wavelength shift induced by cross-phase modulation in highly nonlinear dispersion-shifted fiber," *IEEE Photon. Technol. Lett.*, vol. 17, no. 2, pp. 423–425, Feb. 2005.

[10] J. Li, M. Westlund, H. Sunnerud, B.-E. Olsson, M. Karlsson, and P. A. Andrekson, "0.5-Tb/s eye-diagram measurement by optical sampling using XPM-induced wavelength shifting in highly nonlinear fiber," *IEEE Photon. Technol. Lett.*, vol. 16, no. 2, pp. 566–568, Feb. 2004.

[11] G. P. Agrawal, P. L. Baldeck, and R. R. Alfano, "Temporal and spectral effects of cross-phase modulation on copropagating ultrashort pulses in optical fibers," *Phys. Rev. A*, vol. 40, no. 9, pp. 5063–5072, 1989.

[12] J. W. Lou, J. K. Andersen, J. C. Stocker, M. N. Islam, and D. A. Nolan, "Polarization insensitive demultiplexing of 100-Gb/s words using a twisted fiber nonlinear optical loop mirror," *IEEE Photon. Technol. Lett.*, vol. 11, no. 12, pp. 1602–1604, Dec. 1999.

[13] J. W. Lou, K. S. Jepsen, D. A. Nolan, S. H. Tarcza, W. J. Bouton, A. F. Evans, and M. N. Islam, "80 Gb/s to 10 Gb/s polarization-insensitive demultiplexing with circularly polarized spun fiber in a two-wavelength nonlinear optical loop mirror," *IEEE Photon. Technol. Lett.*, vol. 12, no. 12, pp. 1701–1703, Dec. 2000.

[14] T. Tanemura, J. Suzuki, K. Katoh, and K. Kikuchi, "Polarization-insensitive all-optical wavelength conversion using cross-phase modulation in twisted fiber and optical filtering," *IEEE Photon. Technol. Lett.*, vol. 17, no. 5, pp. 1052–1054, May 2005.

[15] T. Tanemura and K. Kikuchi, "Circular-Birefringence fiber for nonlinear optical signal processing," *J. Lightwave Technol.*, vol. 24, no. 11, pp. 4108–4119, 2006.

[16] K. Utchiyama, S. Kawanishi, H. Takara, T. Morioka, and M. Saruwatari, "100 Gbit/s to 6.3 Gbit/s demultiplexing experiment using polarisation-independent nonlinear optical loop mirror," *Electron. Lett.*, vol. 30, no. 11, pp. 873–875, 1994.

[17] T. Sakamoto, K. Seo, K. Taira, N. S. Moon, and K. Kikuchi, "Polarization-insensitive all-optical time-division demultiplexing using a fiber four-wave mixer with a peak-holding optical phase-locked loop," *IEEE Photon. Technol. Lett.*, vol. 16, no. 2, pp. 563–565, Feb. 2004.
[18] R. Calvani, F. Cisternin, R. Girardi, and E. Riccardi, "Polarisation independent all-optical demultiplexing using four wave mixing in dispersion shifted fibre," *Electron. Lett.*, vol. 35, no. 1, pp. 72–73, 1999.
[19] K. K. Chow, C. Shu, C. Lin, and A. Bjarklev, "Polarization-insensitive widely tunable wavelength converter based on four-wave mixing in a dispersion-flattened nonlinear photonic crystal fiber," *IEEE Photon. Technol. Lett.*, vol. 17, no. 3, pp. 624–626, Mar. 2005.
[20] H. C. Lim, T. Sakamoto, and K. Kikuchi, "Polarization-independent optical demultiplexing by conventional nonlinear optical loop mirror in a polarization-diversity loop configuration," *IEEE Photon. Technol. Lett.*, vol. 12, no. 12, pp. 1704–1706, Dec. 2000.
[21] T. Yang, C. Shu, and C. Lin, "Depolarization technique for wavelength conversion using four-wave mixing in a dispersion-flattened photonic crystal fiber," *Opt. Exp.*, vol. 13, pp. 5409–5415, 2005.
[22] B.-E. Olsson and P. A. Andrekson, "Polarization-independent all-optical AND-gate using randomly birefringent fiber in a nonlinear optical loop mirror," presented at the Opt. Fiber Commun. '98 Conf., San Jose, CA.
[23] T. Okuno, M. Onishi, T. Kashiwada, S. Ishikawa, and M. Nishimura, "Silica-based functional fibers with enhanced nonlinearity and their applications," *J. Sel. Topics Quantum. Electron.*, vol. 5, no. 5, pp. 1385–1391, 1999.
[24] H. C. Nguyen, K. Finsterbusch, D. J. Moss, and B. J. Eggleton, "Dispersion in nonlinear figure of merit of As/sub 2/Se/sub 3/ chalcogenide fibre," *Electron. Lett.*, vol. 42, no. 10, pp. 571–572, 2006.
[25] T. Hasegawa, T. Nagashima, S. Ohara, and N. Sugimoto, "High nonlinearity bismuth fibers and their applications," presented at the Opt. Fiber Commun.' 06 Conf., Anaheim, CA.
[26] K. P. Hansen, "Dispersion flattened hybrid-core nonlinear photonic crystal fiber," *Opt. Exp.*, vol. 11, no. 13, pp. 1503–1509, 2003.
[27] N. Sugimoto, T. Nagashima, T. Hasegawa, S. Ohara, K. Taira, and K. Kikuchi, "Bismuth-based optical fiber with nonlinear coefficient of 1360 $W^{-1}km^{-1}$," presented at the Opt. Fiber Commun. Conf. (PDP26), Los Angeles, CA, Feb. 2004.
[28] K. P. Hansen, A. Petersson, J. R. Folkenberg, M. Albertsen, and A. Bjarklev, "Birefringence-induced splitting of the zero-dispersion wavelength in nonlinear photonic crystal fibers," *Opt. Lett.*, vol. 29, no. 1, pp. 14–16, 2004.
[29] C. D. Poole and D. L. Favin, "Polarization-mode dispersion measurements based on transmission spectra through a polarizer," *J. Lightwave Technol.*, vol. 12, no. 6, pp. 917–929, 1994.
[30] S. Kumar, A. Selvarajan, and G. V. Anand, "Nonlinear copropagation of two optical pulses of different frequencies in birefringent fibers," *J. Opt. Soc. Amer. B*, vol. 11, no. 5, pp. 810–817, May 1994.
[31] F. Yaman, Q. Lin, and G. P. Agrawal, "A novel design for polarization-independent single-pump fiber-optic parametric amplifiers," *IEEE Photon. Technol. Lett.*, vol. 18, no. 22, pp. 2335–2337, Nov. 2006.
[32] A. S. Lenihan, R. Salem, T. E. Murphy, and G. M. Carter, "All-optical 80 Gb/s time-division demultiplexing using polarization-insensitive cross-phase modulation in photonic crystal fiber," *IEEE Photon. Technol. Lett.*, vol. 18, no. 12, pp. 1329–1331, Jun. 2006.
[33] Z. Wang, N. Deng, C. Lin, and C.-K. Chan, "Polarization-insensitive widely tunable wavelength conversion based on four-wave mixing using dispersion-flattened high-nonlinearity photonic crystal fiber with residual birefringence," presented at the ECOC '06 Conf., Cannes, France.
[34] W. Astar, A. S. Lenihan, and G. M. Carter, "Polarization-insensitive wavelength conversion by FWM in a highly nonlinear PCF of polarization scrambled, 10 Gb/s RZ-OOK and RZ-DPSK signals," *IEEE Photon. Technol. Lett.*, vol. 19, no. 20, pp. 1676–1678, Oct. 15, 2007.
[35] R. Salem, A. S. Lenihan, G. M. Carter, and T. E. Murphy, "160 Gb/s polarization-independent optical demultiplexing in 2-m bismuth-oxide fiber," *IEEE Photon. Technol. Lett.*, vol. 18, no. 21, pp. 2245–2247, Nov. 1, 2006.
[36] Q. Lin and G. P. Agrawal, "Vector theory of cross-phase modulation: Role of nonlinear polarization rotation," *J. Quantum Electron.*, vol. 40, no. 7, pp. 958–964, 2004.
[37] C. Ito, S. H. Chung, I. Monfils, and J. C. Cartledge, "Polarization independent all-optical retiming based on cross-phase modulation and spectral slicing," presented at the Opt. Fiber Commun. '07 Conf., Anaheim, CA.
[38] B.-E. Olsson, P. Ohlen, L. Rau, and D. J. Blumenthal, "A simple and robust 40-gb/s wavelength converter using fiber cross-phase modulation and optical filtering," *IEEE Photon. Technol. Lett.*, vol. 12, no. 7, pp. 846–848, Jul. 2000.

Reza Salem (M'06) received the B.S. degree in electrical engineering from Sharif University of Technology, Tehran, Iran, in 2001, and the M.S. and Ph.D. degrees in electrical engineering from the University of Maryland, College Park, MD, in 2003 and 2006, respectively.

He is currently a Postdoctoral Research Associate at Cornell University, Ithaca, NY. His current research interests include nonlinear optics, silicon photonics, and optical communication.

Dr. Salem is a member of the Optical Society of America.

Anthony S. Lenihan (M'96) received the B.S. degree in applied physics from Xavier University, Cincinnati, OH, in 1995, and the M.S. and Ph.D. degrees in electrical engineering from the University of Michigan, Ann Arbor, in 1997 and 2002, respectively.

From 2001 to 2007, he was a member of the research faculty at the University of Maryland Baltimore County, Baltimore, where he was engaged in the experimental research on fiber optic communication systems, nonlinear fibers for optical signal processing, and polarization effects in optical fibers. In 2007, he joined Ziva Corporation, San Diego, CA, where he is currently a research staff.

Dr. Lenihan is a member of the Optical Society of America.

Gary M. Carter (M'82–SM'85) received the Ph.D. degree in physics from Massachusetts Institute of Technology (MIT), Cambridge, in 1975.

He was with MIT's Lincoln Laboratory, where he was engaged in the area of infrared radar, infrared nonlinear optics, and coherent optical communications. He was with the General Telephone and Electronics Corporate Research Laboratories, where he was engaged in the investigation of ultrafast processes in polymers. Since 1988, he has been with the Electrical Engineering Faculty, University of Maryland Baltimore County, Baltimore. His current research interests include modelocked lasers, biosensors, and high-speed optical communications.

Thomas E. Murphy (M'94–SM'07) received the joint B.A./B.S.E.E. degrees in physics and electrical engineering from Rice University, Houston, TX, in 1994, the M.S. and Ph.D. degrees from Massachussetts Institute of Technology, Cambridge in 1997 and 2000, respectively, both in electrical engineering.

In 1994, he joined the NanoStructures Laboratory at Massachusetts Institute of Technology (MIT), where he was engaged in integrated optics and nanotechnology. In 2000, he joined MIT Lincoln Laboratory as a staff member in the Optical Communications Technology Group, where he studied and developed ultrafast optical communications systems. In August 2002, he joined the University of Maryland, College Park, where he is currently an Assistant Professor in the Department of Electrical and Computer Engineering. His current research interests include optical communications, short-pulse phenomena, numerical simulation, optical pulse propagation, nanotechnology, and integrated photonics.

Dr. Murphy is a member of the Optical Society of America (OSA). He is also the recipient of the National Science Foundation (NSF) CAREER Award.